Journal of Physics: Conference Series **498** (2014) 012011 doi:10.1088/1742-6596/498/1/012011

Modelling of waves propagation on irregular surfaces using ray tracing and GTD approaches: Application to head waves simulation in TOFD inspections for NDT

Adrien Ferrand[1], Michel Darmon[1], Sylvain Chatillon[1], Marc Deschamps[2]

[1] CEA, LIST, Department Imaging and Simulation for NDT, 91191 Gif-sur-Yvette cedex, France.
[2] Univ. Bordeaux, I2M–APy, UMR 5295, 33400 Talence, France.

Email : michel.darmon@cea.fr

Abstract. The Time of Flight Diffraction (TOFD) technique is a classical ultrasonic method used in ultrasonic non-destructive evaluation, which allows a precise positioning and a quantitative size evaluation of cracks in the inspected material. Among the typical phenomena arising in the current TOFD inspection, the so-called "head wave" is the first contribution reaching the receiver. The head wave propagation on a planar interface is well known and identified as a critical refraction taking place on the material surface. On irregular surfaces, it has been shown that the head wave results from the melting of surface and bulk waves mechanisms and that surface irregularities are responsible for numerous diffractions of the incident head wave. To simulate such behaviour, a model has been developed using a ray tracing technique based on time of flight minimization (generalized Fermat's principle). It enables the calculation of the ray path and the corresponding time of flight of all waves propagating in the material, including the head wave. To obtain a complete propagation model for these waves (both trajectory and amplitude), the integration of Geometrical Theory of Diffraction (GTD) models is currently performed by coupling them with the ray-based approach discussed above.

1. Introduction

Among the various NDE inspections techniques, the Time of Flight Diffraction (TOFD) technique allows a precise and quantitative evaluation of surface breaking or embedded cracks. This technique uses two ultrasonic probes which are mechanically associated and remote from each other. In a contact inspection, the two probes are positioned on the surface of the inspected specimen using a wedge to ensure the impedance adaptation between the probes and the specimen. The first probe emits an ultrasonic pulse in the specimen, and the second probe receives the diffracted signals arising from the specimen. In Fig. 1, a schematic example of a TOFD inspection on a specimen with a planar surface is provided.

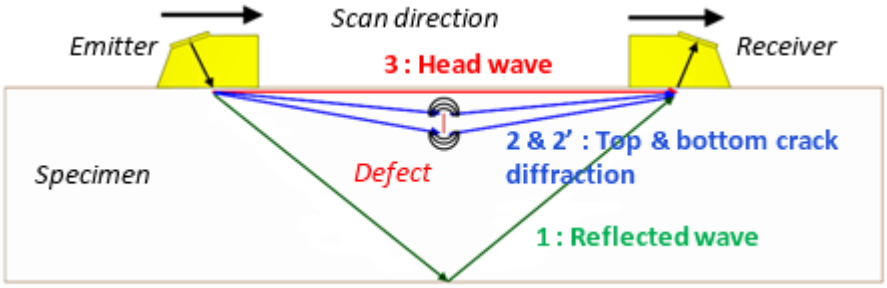

Figure 1. TOFD inspection on a specimen with a planar surface.

Typical waves received by the second probe and their ray representation are shown in Fig. 1. Among these contributions, specular reflections on the bottom of the specimen and diffraction on the defect edges are received. But a wave, represented in Fig. 1 and named the head wave, is detected chronologically before any other. This wave, generated by a critical refraction at the angle between the wedge and the specimen, propagates along the entry surface and finally give rise to a critical radiation from the specimen to the receiver wedge. The principle of head wave propagation along a planar surface separating two fluid media of respective density (and L-wave velocity ( ) is summed up in Fig. 2. The L-wave emitted from the source point is critically refracted at the point A, and critically radiated from the surface at the point B towards the observation point.

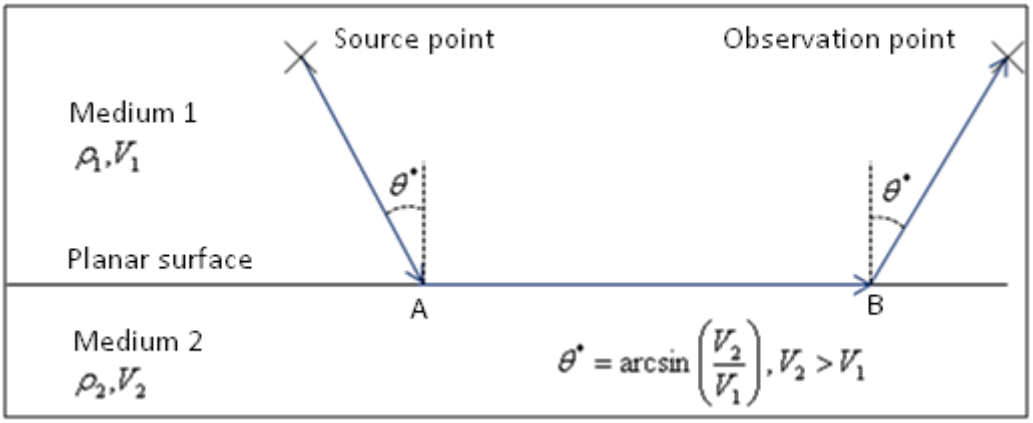

Figure 2. Head wave propagation principle along a planar interface.

The head wave has been historically studied in geophysics. Indeed, seismic inspections often involve stratified media which allow head wave generation on the media interfaces [1]. Analytical models have been developed in the case of stratified media separated by planar interfaces [1], [2], [3], [4]. One of these models [4] is based on a ray approach and asymptotical expansion of the propagation solution: using the hypothesis of a high frequency point source, the head wave propagation can be modeled using a ray approach and can be analytically expressed until the observation point. Furthermore, analytical modelling of the head wave propagation on irregular surfaces has also been proposed in several seismic studies. Indeed, using an integral representation, the received head wave signal has been evaluated for rough surfaces or slightly curved surfaces [5,6] and for spherically symmetric radially heterogeneous media [7]. Some numerical studies [8] have also been performed concerning more generally irregular surfaces and have shown some effects of the irregular surface on the head wave amplitude and time of

flight.The objective of this study is to extend the head wave modeling from the planar interfaces case to the irregular interfaces case using a ray approach in the NDE domain.

The irregular interfaces studied in this work are the scoured surfaces of metal specimens. Scoured surfaces are the result of a specimen repair process. When a defect is detected by a first TOFD inspection near the specimen surface, the matter around the defect is removed in view to be replaced by clean matter. Before the replacement, a new TOFD inspection is carried out on the resulting scoured surface in order to ensure that the entire defect has been removed. During the new TOFD inspection, the measured head wave signal is modified compared to the first TOFD inspection. To understand the differences between the two head wave signals, a test specimen has been designed. This specimen shown in Fig. 3a has a surface divided in two parts: one is planar, the other is scoured. A TOFD inspection is made along the surface, and the resulting B-scan is shown in Fig. 3b.

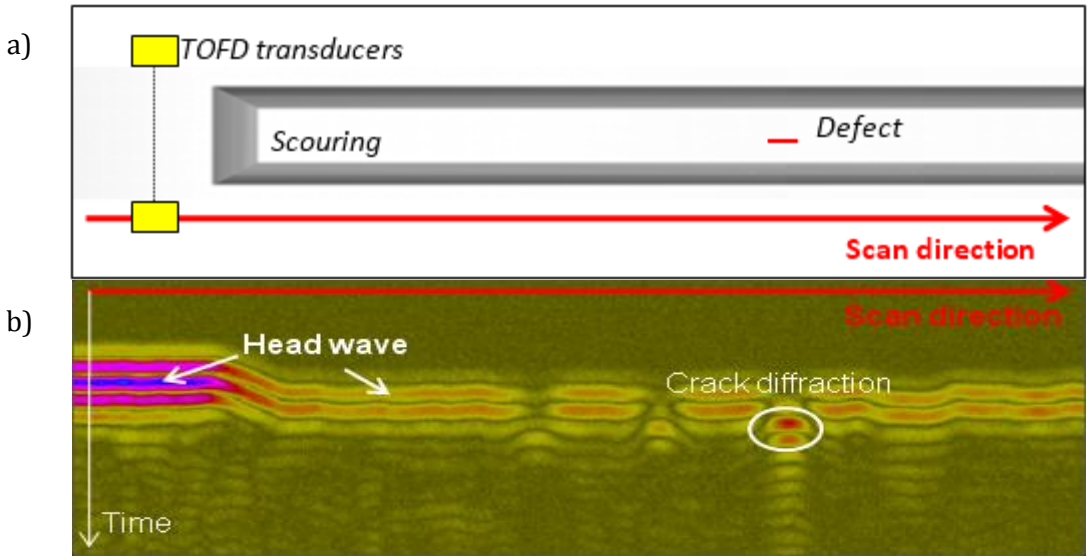

Figure 3. a) Inspection configuration of the test specimen. b) Measured B-scan on both the planar part and the scoured part of the surface

The B-scan obtained during the surface inspection from the planar part to the scoured one represented in Fig. 3, focuses on the effect of the surface irregularity on the head wave signal. In fact, the time of flight of the head wave signal shows that the head wave is delayed when the TOFD transducers reach the scoured part of the surface, which indicates that the head wave propagation is modified. Moreover the head wave signal amplitude measured on the scoured part significantly decreases, (around 20dB) compared with that obtained on the planar part. The modeling of this variation implies the study of head wave scattering by surface irregularities.

The description of the modeling developed in this article is divided in three steps. Firstly, a new ray tracing algorithm has been developed in order to calculate the ray path of the head wave on irregular surfaces (section 2). Secondly, an asymptotic model is proposed to obtain the head wave amplitude on a particular irregular surface (section 3). Finally, some results of a complete model (ray path and amplitude) of the head wave propagation are presented (section 4) for the previously studied surface.

2. Ray modelling of head wave propagation near irregular surfaces

This section is devoted to the description of the developed generic ray tracing tool which allows calculating the head wave path. The head wave scattering on surface irregularities of a specimen

is simulated using the hybrid technique CIVA/Athena [9]. This technique associates the analytical CIVA pencil method for beam modelling and Athena finite elements method (FEM) for beam to scatterer interaction modelling. The results obtained are then considered as a reference to carry out a phenomenological analysis on the scattering effects of the irregular surface. Such an analysis shows that these scattering effects can be interpreted in terms of diffracted rays accordingly to the GTD (Geometrical Theory of Diffraction) principles [10]. The generic ray tracing tool has been developed based on the GTD principles and then validated by comparing its results on the wave ray path with the reference results of CIVA/Athena simulations.

2.1. Interpretation of head wave path near irregular surfaces

In order to interpret the head wave propagation near irregular surfaces, a TOFD inspection simulation has been carried out using the hybrid technique CIVA/Athena on a specimen presenting two flat slopes on its entry surface: these slopes form a corner along the incident surface and correspond to the surface irregularity. The inspection configuration is described Fig. 4.

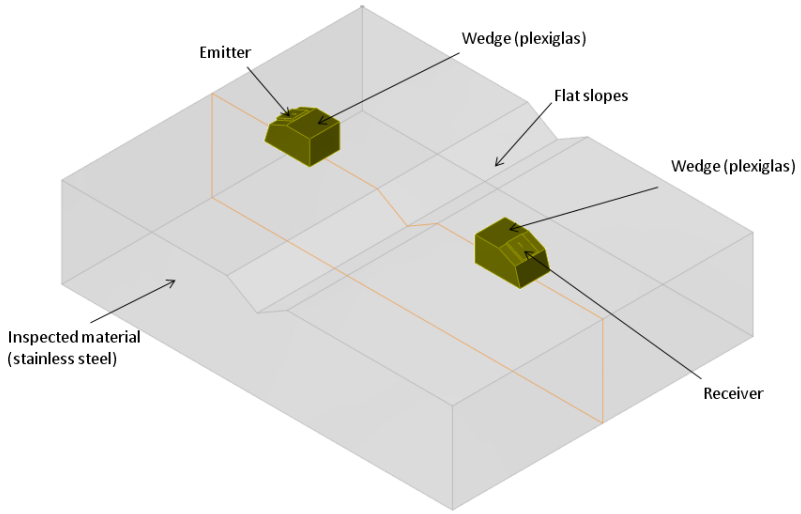

Figure 4. Inspection configuration for the interpretation of the head wave path

The instantaneous elastodynamic field is calculated near the surface irregularities and is represented in Fig. 5. The area near the surface irregularity (a wedge) appears to be divided in two parts: the first one is the specimen area illuminated by the ultrasonic emitted beam and the second one represents the shadow created by the irregularity part. The two parts are separated by the so-called shadow/light boundary whose location is defined by the shape of the surface irregularity and by the emitting transducer position with respect to the surface irregularity. Fig. 5 shows that an elastodynamic field exists in the shadowed area and is damped compared to the one in the insonified area.

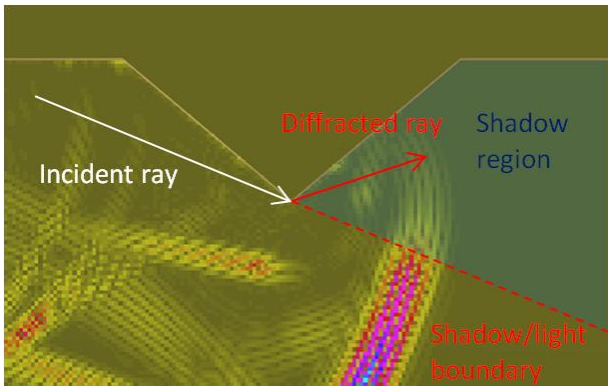

Figure 5. Simulated elastodynamic field around the surface irregularity

In fact, when reached by the incident field, the surface irregularity generates diffraction. The observed diffraction phenomenon corresponds to the canonical problem of wedge diffraction which can notably be predicted by GTD: the wave propagation in the shadowed area can be represented in this case by rays diffracted from the wedge. Moreover the diffracted field generated by the surface irregularities propagates in the specimen and the corresponding wave front reaches the receiver so as to generate the head wave signal received during the TOFD inspection.

Consequently the results of this simulation show that the head wave path is that represented in Fig. 6. The incident ray generated by the contact emitter reaches the entry specimen surface and creates a refracted ray in the specimen. This refracted ray is diffracted on the surface corner into a diffracted ray as predicted by GTD. Then the diffracted ray propagates in the specimen and is then refracted at the interface between the entry specimen surface and the receiver wedge and reaches the receiver crystal.

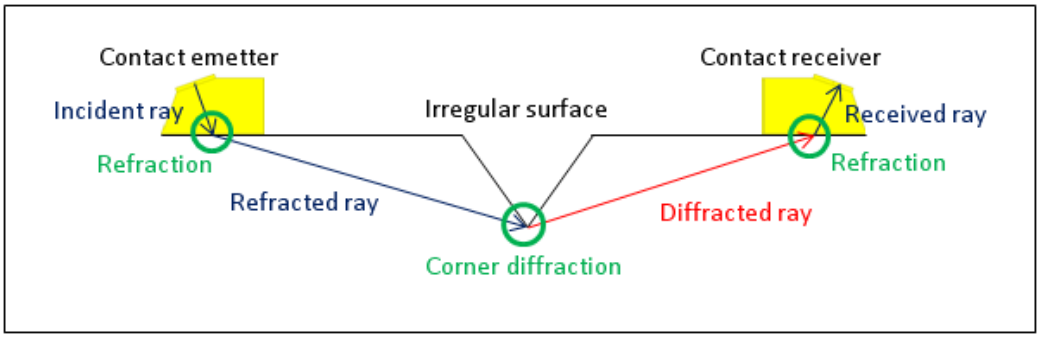

Figure 6. Head wave ray path along the corner surface irregularity

In conclusion the ray approach from the GTD principles is able to interpret the head wave propagation near irregular surfaces, and has been retained to develop the head wave modeling.

2.2. Development of a generic ray tracing tool

A generic ray tracing tool has been developed in order to calculate the head wave path as described in section 3.1. This generic ray tracing tool uses one basic GTD principle, the Generalized Fermat's Principle, whereby a ray path must satisfy the principle of stationary time of flight in order to represent the wave propagation. The Generic Ray Tracing Tool (GRTT) accounts of diffraction from the surface irregularities of the inspected specimen and is able to

simulate paths of all propagating waves including head waves. The algorithm functionalities and description are the subject of a patent filing [11].

To validate the head wave path calculation obtained by the generic ray tracing tool, similar simulations as those performed in section 3.1 have been carried out on two types of surface irregularities: the first one concerns the same specimen as in Fig. 4 which presents two flat slopes on the entry surface, and in the second one shown in Fig. 7b the flat slopes are replaced by cylindrical ones. The elastodynamic field near the surface irregularities and the head wave front is simulated by both GRTT and the FEM hybrid method. Ray paths implying a diffraction of the head wave from the surface irregularities have been calculated in the specimen bulk with the generic ray tracing tool in order to build the theoretical head wave front showing the diffraction effect also predicted by GTD. Thus the GRTT validation consists in comparing the simulated head wave fronts calculated by both hybrid technique CIVA/Athena and GRTT. The comparison is shown in Fig. 7 for the two specimens.

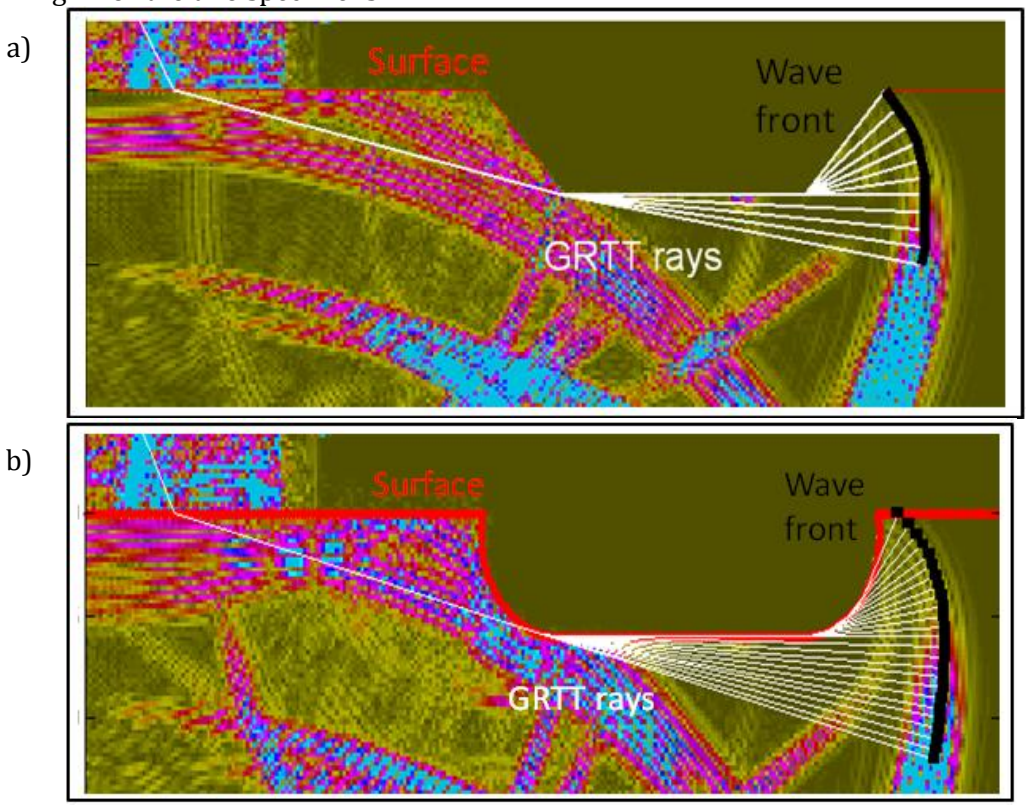

Figure 7. Rays and wave front calculated by GRTT compared to the elastodynamic field (on colours maps) calculated by CIVA/Athena for : a) a specimen with corners, b) a specimen with curved surfaces

As observed in Fig. 7, the theoretical head wave fronts calculated in the two specimens are in good agreement with the diffracted wave fronts obtained with the hybrid technique CIVA/Athena. The comparisons done in the bulk specimen validate the GRTT ray approach used to simulate the diffractions effects responsible of the head wave propagation near irregular surfaces.

3. Development of GTD models for head waves amplitude on curved surface irregularities

The GRTT described in section 3 provides the ray and time of flight of the head wave. Now the calculation of the head wave amplitude with GTD models using the knowledge of the ray path is described. To this aim, the GTD approach is used: it refers to mathematical methods of asymptotical developments [8,9] which allow a complete calculation of the head wave amplitude by the study step by step of the diffraction effects along the head wave ray path.

3.1. Principle of amplitude calculation along a ray-based model

Ray path calculated by GRTT is composed of one or more diffracted or specular rays connected to each other. Each ray composing the ray path must be studied independently to calculate the total amplitude of the wave propagating along the ray path. Indeed the GTD approach expresses the amplitude carried by a ray as follows: for a ray of length *r*, the displacement on the ray extremity is given by the amplitude model:

$$u_d(r) = \mathrm{A}_{source} \exp(i\psi_{source}) \quad D \quad L(r) \quad \exp(ikr) \tag{1}$$

where $\mathrm{A}_{source} \exp(i\psi_{source})$ is the amplitude carried by the incident ray, D is the diffraction coefficient depending on the nature of the effect responsible of the ray launching, $L(r)$ is the divergence factor of the ray, and $\exp(ikr)$ is the phase factor of the ray (k being the wave number). The previous formula shows that GTD expresses the amplitude of a ray as the product of the incident field $\mathrm{A}_{source} \exp(i\psi_{source})$ and of a scattering term $D \quad L(r) \quad \exp(ikr)$ which depends on the nature of the ray (diffracted in the bulk from an irregularity, creeping…) and on its geometrical characteristics.

The approach for a single ray is generalized in order to obtain the amplitude of a wave propagating along a ray path with the following algorithmic principle. An example is given on the Fig. 8. Firstly, the GRTT is used to generate the ray path of the head wave between the known source and observation points. Then the wave propagation is studied along the ray path in order to detect all the interactions between the wave and the surface. Each interaction i generates the ray i with the corresponding amplitude model (with the associated scattered displacement $u_d^{(i)}(r_i)$) which depends on the nature of the interaction, the geometrical parameters of the ray i and the incident field $u_d^{(i-1)}(r_{i-1})$ coming from the ray $i-1$. Finally the total amplitude of the wave propagating along the ray path on the observation point is given by the concatenation of all the amplitude models:

$$u(P_{observation}) = f(u_d^{(1)}(r_1), u_d^{(2)}(r_2), \ldots, u_d^{(n)}(r_n)) \tag{2}$$

$$u(P_{observation}) = u(\mathrm{P}_{source}) \prod_{i=1}^{n} D_i \left[\sqrt{d\Sigma(r_i') / d\Sigma(r_i)} \right] \exp(ikr_i) \tag{3}$$

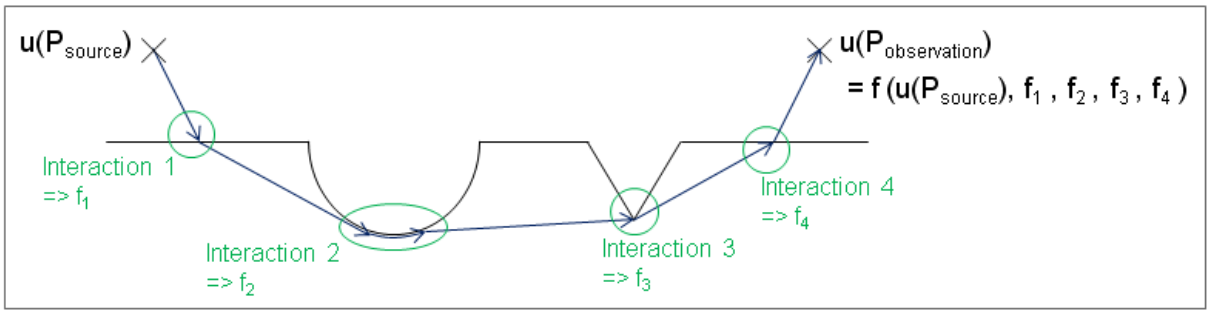

Figure 8. Example of an amplitude calculation along a ray path calculated by GRTT

The amplitude calculation of a wave along a ray path is then made by the application of adapted amplitude models on each ray composing the ray path. These models are asymptotic ones (GTD) and one model will now be presented for a specific diffraction effect occurring in TOFD inspection near irregular surfaces: the diffraction of the head wave on a curved surface irregularity.

3.2. Principle of amplitude calculation along a ray-based model

The head wave ray path calculated by GRTT in specimens with curved surfaces irregularities has been presented in Fig. 7b. It shows a particular diffraction along the irregularities which is presented in Fig. 9 for the case of a cylindrical one with a point source S and an observation point located on Q. It appears that the ray path integrates a bulk ray SP_1 which is tangentially incident to the curved surface irregularity and launch a surface ray P_1P_2 along this irregularity. After the surface propagation, this ray generates a diffracted bulk ray P_2Q tangentially to the irregularity in the shadow region formed by the surface. The ray P_1P_2 is predicted by the GTD and is called a creeping ray.

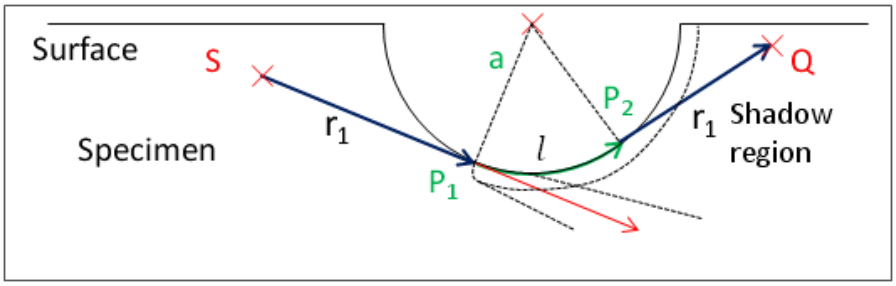

Figure 9. Creeping ray path along an cylindrical surface irregularity

The amplitude of the wave propagating along the path SP_1P_2Q results from the diffraction of the creeping ray P_1P_2 in the shadow region. The corresponding chosen creeping ray amplitude model derivates from the canonical problem of plane wave diffraction from a soft cylinder of radius a using an asymptotic expression of the solution only valid for a scalar wave at high frequency in the shadow region of the cylinder (mode conversions of elastic case are neglected). For a line source (2D approximation) S emitting at the wave number k, this model [13] gives the following amplitude:

$$u(Q) = D_S \frac{e^{ikr_1}}{\sqrt{r_1}} \sum_{n=0}^{\infty} D_{sr,cr}^{(n)} D_{cr,sr}^{(n)} e^{i\frac{\nu_n}{a}l} D_S \frac{e^{ikr_2}}{\sqrt{r_2}} \tag{4}$$

With D_S the dyadic source coefficient equal to $e^{i\pi/4}/\sqrt{8\pi k}$, the first term $D_S \dfrac{e^{ikr_1}}{\sqrt{r_1}}$ is the incident ray SP_1 amplitude and the last term $D_S \dfrac{e^{ikr_2}}{\sqrt{r_2}}$ is the diffracted ray P_1Q amplitude generated by the creeping ray. The term $\sum_{n=0}^{\infty} D_{sr,cr}^{(n)} D_{cr,sr}^{(n)} e^{i\frac{\nu_n}{a}l}$ is the asymptotic expansion of the creeping ray model and includes the diffraction effect on the curved surface. Indeed, $D_{sr,cr}^{(n)}$ and

$D_{cr,sr}^{(n)}$ are respectively the attachment and detachment coefficients on P_1 and P_2 of the creeping ray and can be expressed using first order Airy functions:

$$D_{sr,cr}^{(n)} D_{cr,sr}^{(n)} = D_n^2 = \frac{2^{2/3} e^{-i\pi/6} (ka)^{1/3}}{\left[A_i'(-\bar{\eta}_n) \right]^2}, \tag{5}$$

where $\bar{\eta}_n$ are the zeros of the Airy function. Furthermore the ν_n term of the asymptotic expansion is the attenuation term of the creeping ray which represents the energy loss due to the diffraction in the bulk during the creeping ray propagation. ν_n is expressed using the zeros $\bar{\eta}_n$ of the Airy function:

$$\nu_n = ka + \left(\frac{ka}{2} \right)^{1/3} e^{i\pi/3} \bar{\eta}_n \tag{6}$$

4. Simulated results

The creeping ray amplitude model has been evaluated by a parametric study of the asymptotic expansion $\sum_{n=0}^{\infty} D_{sr,cr}^{(n)} D_{cr,sr}^{(n)} e^{i\frac{\nu_n}{a}l}$ presented in section 3.1. The two significant parameters of the model are the radius of curvature a of the curved irregularity and the frequency of the head wave. For a fixed creeping ray length of 10 mm, the Fig. 10 presents the results of the parametric study for typical values of a and f encountered in TOFD inspections.

a)

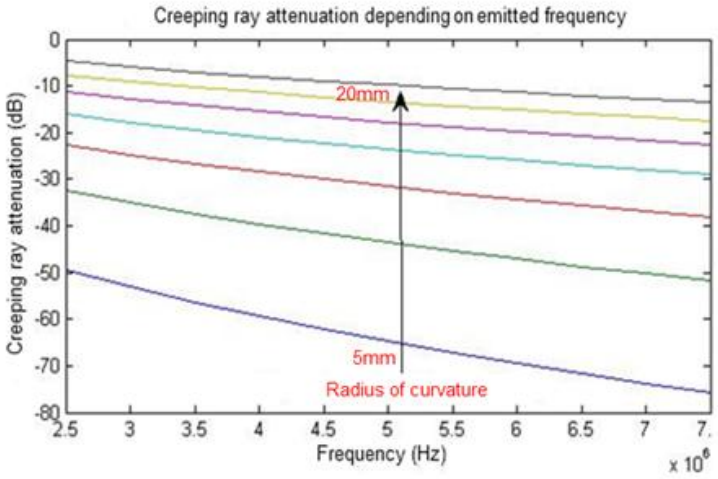

b)

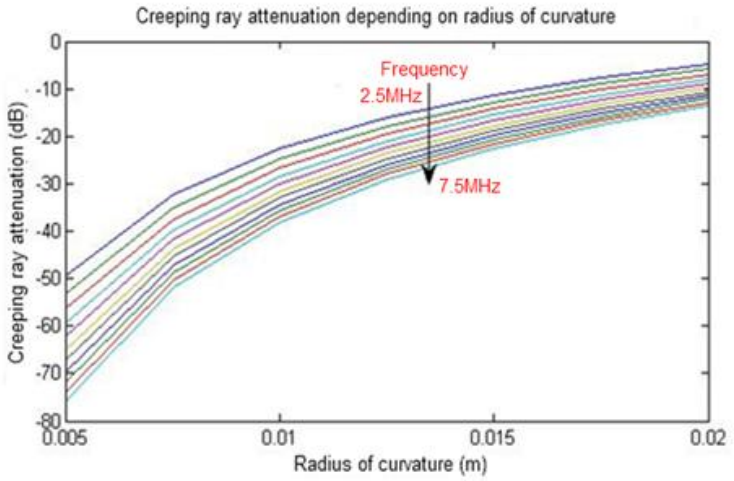

Figure 10. Results for the parametrical study of the asymptotic expansion : wave attenuation over frequency (a) and radius of curvature (b)

The parametric study shows that the wave propagation along a creeping ray implies a strong attenuation of its amplitude.

The amplitude calculation approach of section 3.1 has been followed to integrate the creeping ray amplitude model in the GRTT and to obtain a complete simulation of head wave fronts propagating along curved surfaces irregularities. Some simulations have been then carried out on the specimen presented in Fig. 8 (for a radius curvature of the irregularity of 10 mm and a harmonic line source of frequency 5MHz): the GTD creeping ray model presented in section 3 has been used in the shadow area formed by the cylindrical surface irregularity and the wave in the insonified area has been simulated using the classical results of Geometrical Acoustics. The calculated wave fronts for different steps of the propagation are shown in Fig. 11. The amplitude carried by the rays is represented using a color code with a reference amplitude equal to the mean amplitude of the front in the specimen before reaching the surface irregularity.

a)

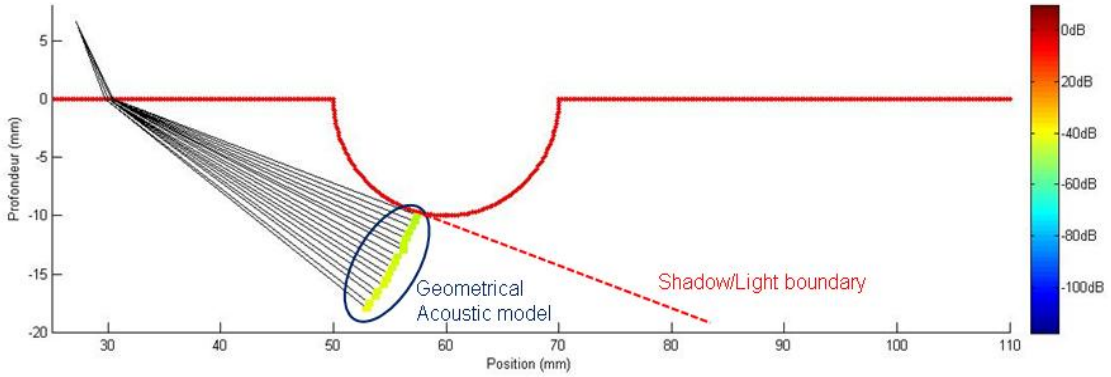

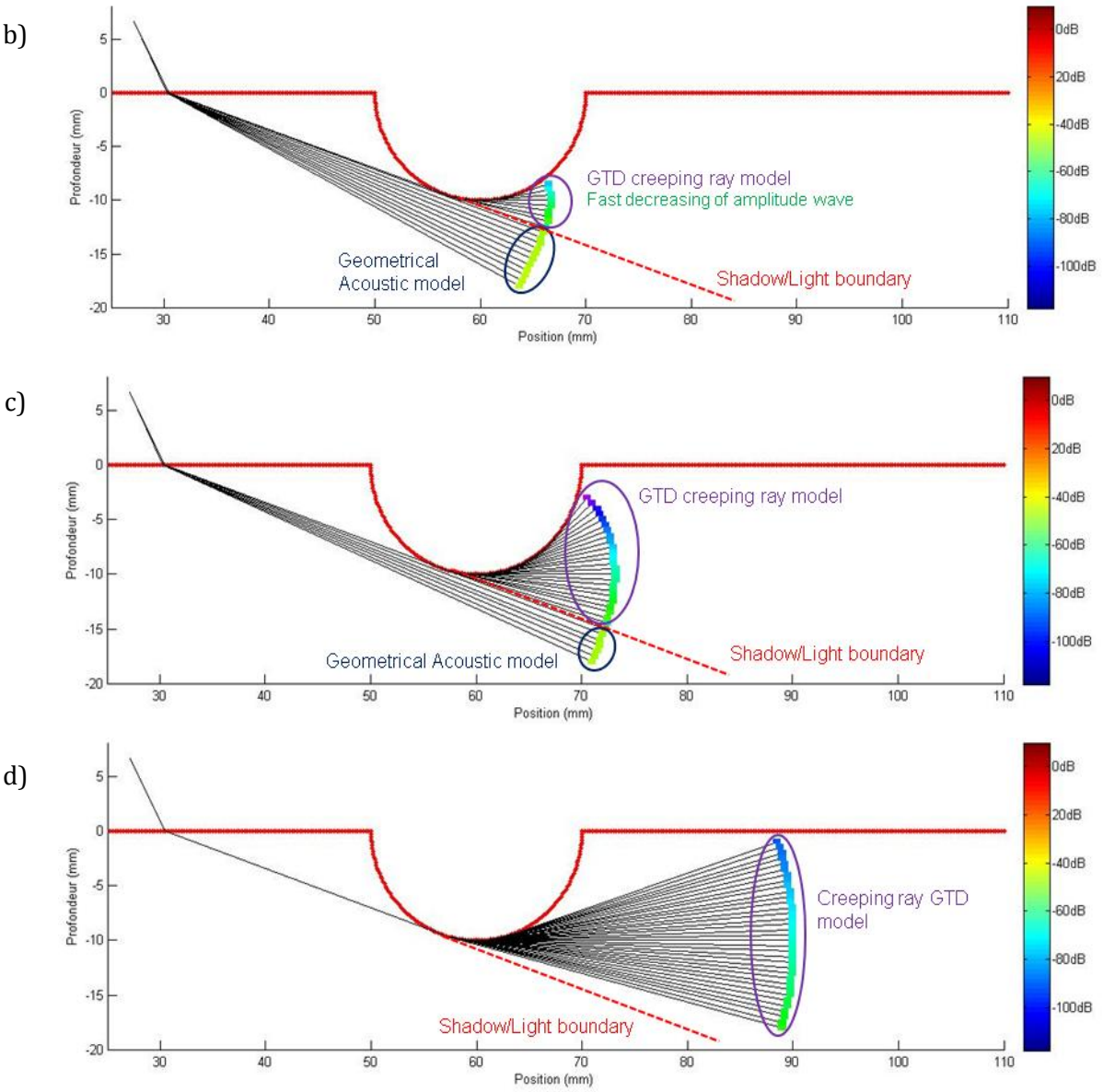

Figure 11. Complete simulation (ray paths and amplitude) of the wave front by the GRTT at different steps of the propagation (a, b, c, d)

The curved surface irregularity forms a shadow area (Fig. 11a) in which the head wave is diffracted from the irregularity. In the shadow area, the creeping ray model is applied (Fig. 11b, 11c). The resulting simulation shows that the head wave front in the shadow area is strongly attenuated during its propagation (Fig. 11d). Far from the irregularity, the amplitude attenuation in the shadow zone is of 20dB to 40dB compared to the insonified zone. The complete simulation of the head wave including ray path, time of flight, wave front and amplitude is thus done for the case of cylindrical surface irregularities.

Conclusion

Classical models of head waves along planar surfaces cannot be used to simulate head waves along irregular surfaces in TOFD inspection. Whereas the head wave behavior on planar surfaces

postulates a surface propagation, head waves on irregular surfaces are the result of both surface and bulk propagation.

In order to simulate the head wave propagation in such irregular surfaces by a ray approach, a generic ray tracing tool (GRTT) has been developed to model the diffraction phenomena predicted by the Geometrical Ray Theory, arising along the surface irregularities and responsible of the head wave propagation. The GRTT has been validated concerning the ray path and the time of flight of head waves. Moreover specifics GTD models using asymptotic developments have been integrated to calculate the head wave amplitude and then provide a complete simulation of the head wave on cylindrical surface irregularities for TOFD inspections.

References

[1] L. M. Brekhovskikh, *Waves in layered media*. Academic Press, 1960.
[2] L. Cagniard, E. A. Flinn, C. H. Dix, and W. G. Mayer, "Reflection and Refraction of Progressive Seismic Waves," *Phys. Today*, vol. 16, p. 64, 1963.
[3] A. De Hoop, "A modification of Cagniard's method for solving seismic pulse problems," *Appl. Sci. Res. Sect. B*, vol. 8, no. 1, pp. 349–356, 1960.
[4] V. Červený and R. Ravindra, *Theory of seismic head waves*. University of Toronto Press (Toronto), 1971.
[5] I. Lerche and N. Hill, "A mean-field solution of the reflection of a spherical acoustic wave from a rough interface," *J. Math. Phys.*, vol. 26, p. 1420, 1985.
[6] I. Lerche, "On the reflection of acoustic waves from a slightly curved interface," *J. Acoust. Soc. Am.*, vol. 81, p. 611, 1987.
[7] D. P. Hill, "Critically refracted waves in a spherically symmetric radially heterogeneous earth model," *Geophys. J. Int.*, vol. 34, no. 2, pp. 149–177, 1973.
[8] H. Zhou and X. Chen, "Ray path of head waves with irregular interfaces," *Appl. Geophys.*, vol. 7, no. 1, pp. 66–73, 2010.
[9] N. Gengembre, A. Lhémery, R. Omote, T. Fouquet, and A. Schumm, "A semi-analytic-FEM hybrid model for simulating UT configurations involving complicated interactions of waves with defects," in *AIP Conference Proceedings*, 2004, vol. 700, p. 74.
[10] J. B. Keller, "Geometrical theory of diffraction," *JOSA*, vol. 52, no. 2, pp. 116–130, 1962.
[11] Patent filing related to GRTT in progress. Its precise reference will be given in the proofs.
[12] D. Bouche, F. Molinet, and R. Mittra, *Asymptotic methods in electromagnetics*. Springer, 1997.
[13] F. Molinet, *Acoustic High-Frequency Diffraction Theory*. Momentum Press, 2011.